Magnetic porous carbons derived from cobalt (II)-based metal-organic frameworks for the solid-phase extraction of sulfonamides

Sandra Yadira Mendiola Alvarez,[1,2] Gemma Turnes Palomino,[2] Jorge Guzmán Mar,[1] Ma. Aracely Hernández Ramírez,[1] Laura Hinojosa Reyes*[,1], Carlos Palomino Cabello[*,2]

[1] *Facultad de Ciencias Químicas, Universidad Autónoma de Nuevo León, UANL, Cd. Universitaria, C.P. 66455 San Nicolás de los Garza, Nuevo León, México*

[2]*Department of Chemistry, University of the Balearic Islands, E-07122 Palma de Mallorca, Spain*

**E-mail: carlos.palomino@uib.es *E-mail: laura.hinojosary@uanl.edu.mx*

ABSTRACT

In this work, the dispersive solid-phase extraction of sulfonamide antibiotics was evaluated using magnetic porous carbon derived from cobalt (II)-based metal-organic frameworks. By direct carbonization under inert atmosphere of Co-SIM-1, Co-MOF-74 and Co-DABCO MOFs, different magnetic porous carbons were prepared and characterized to study their structural, morphological, chemical and textural properties. Their performance for the simultaneous extraction of three sulfonamides (sulfadiazine, sulfamerazine and sulfamethazine), prior to HPLC analysis, was also evaluated, obtaining the best results (> 95%) in the case of C/Co-SIM-1 carbon, probably due to its bimodal pore structure, high surface area and high amount of surface defects. Using this adsorbent, the effect of the pH solution and contact time on the adsorption of the sulfonamides, as well as the reusability of the carbon were studied.

Keywords: Porous carbons, metal-organic frameworks, sulfonamides, magnetic solid-phase extraction, water pollutants.

1. Introduction

The consumption of antibiotics is increasing in both industrialized and developing countries, resulting in their frequent detection in surface waters around the world. Sulfonamides, classified as emerging contaminants (EC), are synthetic broad-spectrum antibiotics, which are widely used in veterinary to inhibit both gram-positive and gram-negative bacteria, as well as some protozoa, and also in animal industry as growth promoters.[1,2] This kind of antibiotics, also known as sulfa drugs, is not biodegradable and, due to their high polarity and water solubility, usually cannot be completely removed from water in conventional water treatment plants, having been detected in some water bodies.[3–5] The long-term effects of low concentrations of these pollutants, due to its biological activity and stability in water, can pose serious risks to human health and to the environment.

Among the various available methods developed to remove organic pollutants, adsorption has emerged as one of the most attractive because of its simplicity, reliability, and cost effectiveness without generating secondary pollutants.[6,7] Owing to their unique characteristics, such as high surface area, variable functionality and tunable pore size and composition, metal-organic frameworks (MOFs) have been applied as adsorbents of different pollutants, including some sulfonamides. For instance, the extraction of sulfamethoxazole by MIL-53 MOFs with different metallic centers[8] or the excellent performance of ZIF-67 and UiO-66 MOFs for the adsorptive removal of sulfachloropyradazine antibiotic in wastewater[9] have been described, while metal-organic frameworks with coordinatively unsaturated sites, such as HKUST-1 and MIL-101, have been studied as efficient sorbents for the adsorption of different sulfonamides.[10,11]

Although many MOFs have been tested on the extraction of organic pollutants, several of them have been described as unstable in aqueous solutions under a wide range of pH conditions, limiting their applicability as adsorbents.[12] In addition, the laborious and time-consuming retrieval of these porous materials from the sample medium, inhibits its direct application for the extraction of organic pollutants in batch conditions.

Recently, stable porous carbons have been prepared by a facile and single-step calcination procedure under inert atmosphere without the need of any additional carbon precursor using metal-organic frameworks as both templates and carbon precursors.[13,14] The high porosity, defined structure and outstanding designability of MOFs allow a precise control of the size, structure, morphology and composition of the MOF-derived porous carbon. The obtained carbons are uniform doped with heteroatoms from the organic linkers, which can act as active sites, show excellent chemical and thermal stability, high porosity and hydrophobicity which makes them good candidates as sorbents for the removal of organic pollutants.[15–17] Furthermore, bearing in mind that after the carbonization process the metallic component of the MOF aggregates, shaping metal or metal oxide nanoparticles, the use of iron, nickel, and cobalt based MOFs as precursors to prepare porous carbons, results in magnetic porous carbons, which facilitates their retrieval due to the easy magnetic separation of the adsorbent avoiding filtration or centrifugation steps.[18–21]

Thus, the aim of this work is to explore the use of magnetic porous carbons, obtained by simple one-step pyrolysis of different cobalt (II)-based metal-organic frameworks (Co-SIM-1, Co-MOF-74 and Co-DABCO), for the adsorption of sulfonamides (sulfamethazine, sulfamerazine and sulfadiazine). The influence of the pH of the extraction medium on the adsorption mechanism of sulfonamides compounds from water was established and, taking

into account its practical application, kinetics, regeneration and reusability of the carbon showing highest adsorption capacity (C/Co-SIM-1) were also examined. The obtained results demonstrate that the C/Co-SIM-1 is a promising adsorbent for the efficient sulfonamides extraction from water systems.

2. Experimental section

2.1 Chemicals

All chemicals used were of analytical grade. N,N-dimethylformamide (DMF, extrapure) and ethanol (99%) were obtained from Scharlau (Barcelona, Spain). Cobalt(II) nitrate hexahydrate (99%), 4-methyl-5-imidazolecarboxaldehyde (99%), 2,5-dihydroxyterephthalic acid (98%), 1,4-diazabicyclo[2.2.2]octane (DABCO, 98%), sulfamethazine sodium salt (SMTZ, 98%), sulfamerazine (SMRZ, 99%), sulfadiazine (SDZ, 99%), trifluoroacetic acid (TFA, 99%) were purchased from Sigma Aldrich. Acetonitrile (HPLC grade) was obtained from PanReac AppliChem. Methanol (HPLC grade) was acquired from Tedia. Milli-Q water was obtained from a Direct-8 purification system (resistivity > 18 MΩ cm, Millipore Iberica, Spain).

2.2 Instrumentation

The morphology of the prepared materials was examined by scanning electron microscopy using a Hitachi S-3400N microscope, equipped with a Bruker AXS Flash 4010 energy-dispersive X-ray spectroscopy (EDS) system. X-ray diffraction (XRD) patterns were obtained on a Bruker D8-Advanced diffractometer using Cu-Kα radiation (λ = 1.5418 Å) from 5-80° with a step size of 0.02 (2θ). Raman spectra were acquired from 100 to 1000 cm^{-1} on a NRS-5100 (JASCO Co., Japan) using a charge coupled device (CCD) detector at the laser excitation of 785 nm with 10.8 mW laser power. The I_D/I_G ratios were calculated by

measuring the intensity on the band maximum. The nitrogen adsorption/desorption isotherms were collected at 77 K using a micromeritics TriStar II 3020 apparatus (Micromeritics Instrument Corporation). The samples were degassed at 423 K for 12 h using the outgas port of the TriStar II instrument. The isotherms were analyzed by using the Brunauer-Emmett-Teller (BET) method to determine the specific surface area and the two dimensional non-local density functional theory (2D-NLDFT) model for the determination of the pore volume and the pore size distribution. The isoelectric point was measured in a Zetasizer Nano ZS90 (Malvern) by dispersing 5 mg of carbon samples into 10 mL of water at 25 °C and adjusting the pH of the suspension with 0.1 M HCl or 0.1 M NaOH. X-ray photoelectron spectroscopy (XPS) measurements were performed on a PHI 5000 Versa Probe II XPS system using a monochromatic Al Kα X-ray source (hv = 1486.7 eV). The analysis of sulfonamides (SNs) by HPLC was carried out using an HPLC Jasco MD-4017 equipped with a UV-Vis diode array detector. The separation of SNs was carried out by isocratic elution with water acidified with 0.0025% of TFA-acetonitrile (90:10, v/v) on a C18 KINETEX phenomenex® 5 µm (150 × 4.6 mm) column at a flow rate of 0.7 mL/min. The analytes were detected at 230 nm.

2.3 Synthesis of cobalt (II)-based metal-organic frameworks

Co-SIM-1, Co-MOF-74 and Co-DABCO were synthesized by a solvothermal route using experimental conditions previously described.[22–24] Briefly, Co-SIM-1 was prepared by dissolving 3.01 g of 4-methyl-5-imidazolecarboxaldehyde and 1.99 g of cobalt(II) nitrate hexahydrate in 50 mL of DMF under constant stirring. The mixture was introduced into a wide mouth glass jar and heated at 358 K for 72 h. The resulting powder was washed 3 times with DMF and ethanol and then dried at 373 K overnight.

For preparation of Co-MOF-74, 0.75 g of 2,5-dihydroxyterephthalic acid and 3.56 g of cobalt(II) nitrate hexahydrate were added successively to 300 mL of a solution of DMF:ethanol:water (1:1:1, v/v) under constant magnetic stirring, which was maintained for 1 h. The resulting solution was transferred into a wide mouth glass jar and heated at 373 K in an oven for 24 h. After cooling to room temperature, the red solid was filtered and washed 3 times with DMF, and then soaked in methanol for 2 days (the methanol was replaced 4 times during this period). Finally, the solid was filtered and then dried at room temperature under vacuum.

Co-DABCO MOF was synthesized by mixing a cobalt(II) nitrate solution (0.34 g of cobalt(II) nitrate hexahydrate in 10 mL of DMF) with 0.21 g of 2-aminoterephthalic acid dissolved in 10 mL of DMF under stirring. After that, a DABCO solution (0.21 g of DABCO in 10 mL of DMF) was added with constant stirring, that was maintained for 5 h. After this time the solid formed was separated by filtration and the solution was heated at 393 K in a stainless-steel autoclave for 72 h. The resulting powder was washed thoroughly with DMF and dried at room temperature for 12 h.

2.4 Preparation of magnetic carbons

The magnetic porous carbons C/Co-SIM-1, C/Co-MOF-74 and C/Co-DABCO were obtained by direct calcination of 2 g of the synthesized Co-SIM-1, Co-MOF-74 and Co-DABCO, respectively, in a tubular furnace under a nitrogen gas flow at 1073 K (heating rate of 3 K min^{-1}) for 2.5 h. The materials were then cooled to room temperature maintaining the N_2 atmosphere. Finally, the obtained carbons were washed with water and dried under vacuum.

2.5 Solid-phase extraction procedure

The extraction experiments were conducted under batch conditions using 50 mL of sulfonamides (SNs) solutions containing 5 mg/L of each compound (SDZ, SMTZ and SMRZ) and 5 mg of magnetic porous carbon as adsorbent. After 4 h of stirring, an external magnet was placed outside of the sample beaker to separate the sorbent from the aqueous solution, and the non-retained sulfonamides were determined by HPLC-UV analysis. For kinetics studies, a 5 mg/L (each) sulfonamide aqueous solution was mixed with the C/Co-SIM-1 carbon (1 mg/mL) under stirring at pH 5 and the concentration of remaining sulfonamides in solution was measured every 30 minutes. The sorption data were analyzed with a pseudo-second-order adsorption model,[25] whose linearized-integral form is expressed by the following equation:

$$\frac{t}{q_t} = \frac{t}{q_e} + \frac{1}{k_2 q_e^2}$$

where q_t and q_e (mg/g) are the amount of sulfonamide adsorbed at a time t (min) and at equilibrium, respectively, and k_2 is the pseudo-second-order rate constant (g/mg min).

The enrichment factors were determined as the ratio of the peak areas from the HPLC chromatograms before and after the extraction of the sulfonamides using 1 mL of methanol as eluent. The reusability of the material was studied following the procedure described before five times. Between consecutive extractions, the material was washed thoroughly with methanol before being reused in the adsorption process. All the adsorption experiments were carried out in triplicate.

3. Result and Discussions

3.1 Preparation of magnetic porous carbons

In a first step, Co-SIM-1, Co-MOF-74 and Co-DABCO MOFs precursors were synthesized by solvothermal method. The X-ray diffractograms of all the cobalt metal-organic frameworks (Fig. 1a) showed good crystallinity and matched well with the theoretical diffraction patterns previously reported for the same MOF structures,[22,24,26] demonstrating that, in all cases, the corresponding MOF structure was obtained. Fig. 1b shows the diffractograms of C/Co-SIM-1, C/Co-MOF-74 and C/Co-DABCO carbon samples. After the carbonization process, no peaks corresponding to the precursor structure were detected in all cases, while three new peaks at $2\theta = 43°$, 53° and 76° appear in all the diffraction patterns, which were assigned to metallic cobalt particles,[27,28] although the presence of a small fraction of amorphous cobalt oxide cannot be discarded. It should be noted that the width of the peaks assigned to metallic cobalt particles differs from one sample to another, suggesting that the MOF composition affects the size of the cobalt particles formed during the calcination process. In addition, in the case of C/Co-SIM-1, a weak diffraction line at $2\theta = 25°$ was observed, which was assigned to graphitic carbon.[28,29] The degradation of the prepared Co containing MOFs was studied by thermogravimetric analysis (Figure S1). In all cases, the first weight loss before 200 °C is due to the removal of adsorbed solvents, and the second weight loss around 300 °C for Co-DABCO and 400 °C for Co-SIM-1 and Co-MOF-74 is attributed to the decomposition of MOFs structure, indicating the high thermal stability of the precursors. After 800 °C, the mass of the materials was relatively stable. The morphology of the obtained carbons was studied by scanning electron microscopy. As it can be observed in the corresponding SEM micrographs (Fig. 2a-c), the C/Co-SIM-1, C/Co-MOF-74 and C/Co-DABCO samples are formed by micrometer-sized particles with cubic, hexagonal rod and square rod morphology, respectively. Compared to the initial MOFs (Fig. S2), all the derived carbons retained the original shape after the carbonization procedure due to the use

of thermally stable frameworks as precursors.[30,31] Furthermore, elemental EDS mappings (Fig. 2d-e) confirmed that, in all cases, the Co particles were homogeneously distributed on the surface of the obtained carbon.

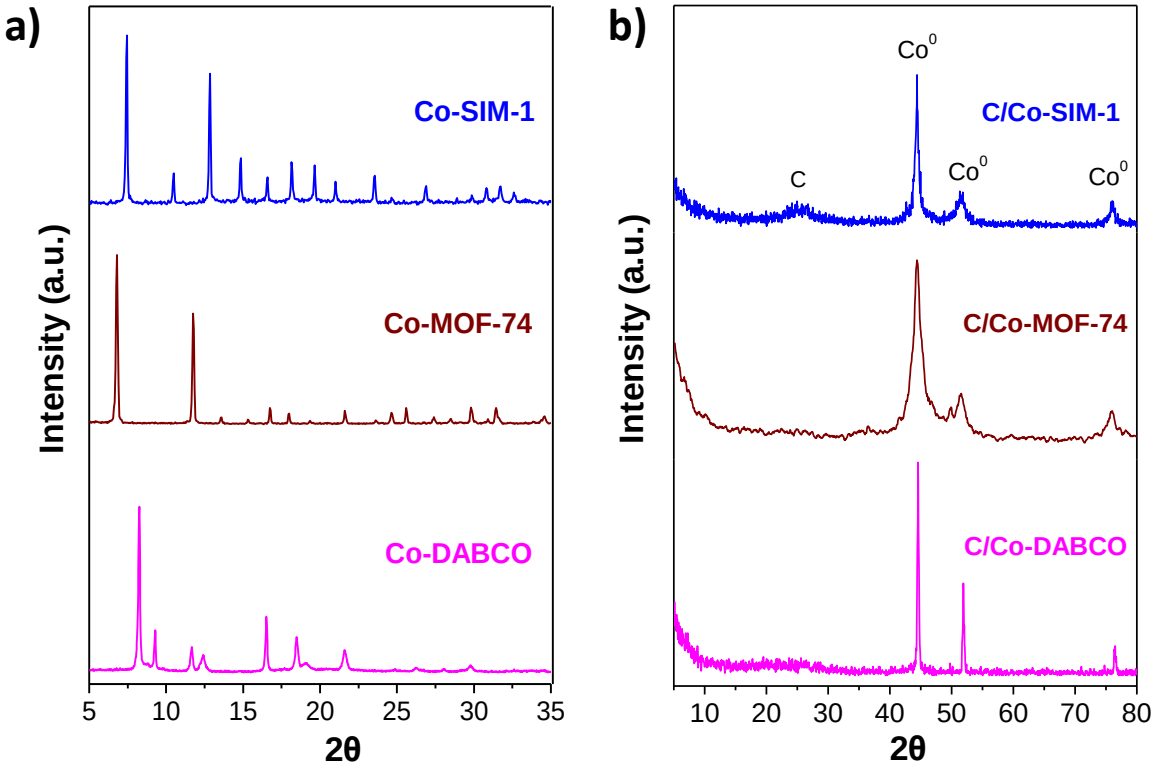

Fig. 1. X-ray diffractograms of (a) Co-SIM-1, Co-MOF-74 and Co-DABCO MOF samples and (b) C/Co-SIM-1, C/Co-MOF-74 and C/Co-DABCO carbon samples.

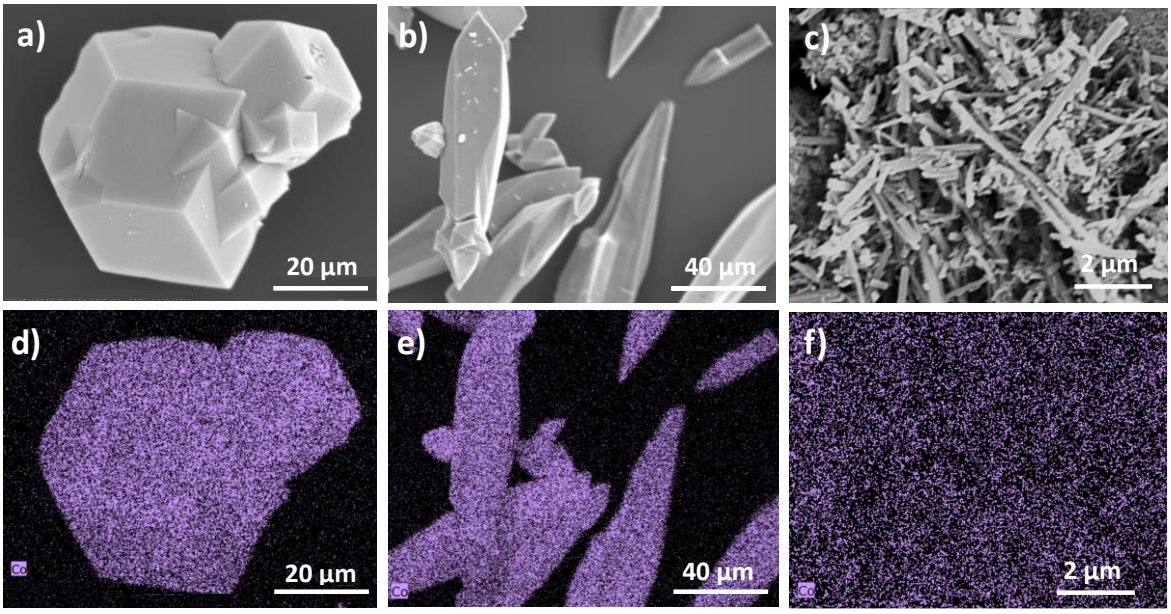

Fig. 2. SEM images and Co EDS mapping of (a,d) C/Co-SIM-1, (b,e) C/Co-MOF-74, and (c,f) C/Co-DABCO samples.

Nitrogen adsorption-desorption isotherms, and the corresponding pore size distribution curves, of the prepared carbon samples are shown in Fig. 3. All carbonaceous materials showed a significant nitrogen uptake at lower P/P_0 values (<0.1) and a hysteresis loop (Fig. 3a), which indicate the simultaneous presence of micropores and mesopores.[32] The determined BET surface areas ranged from 261 to 361 m^2/g (Table 1), which are lower than those of precursor MOFs (between 1213 and 373 m^2/g) due to a partial collapse of the structure during the carbonization process. The pore size distributions calculated using the 2D-NLDFT model (Fig. 3c), corroborated, in all the cases, the coexistence of micropores, with a diameter centered around 10 Å, and mesopores with a broad size distribution (Fig. 3b and Table 1).

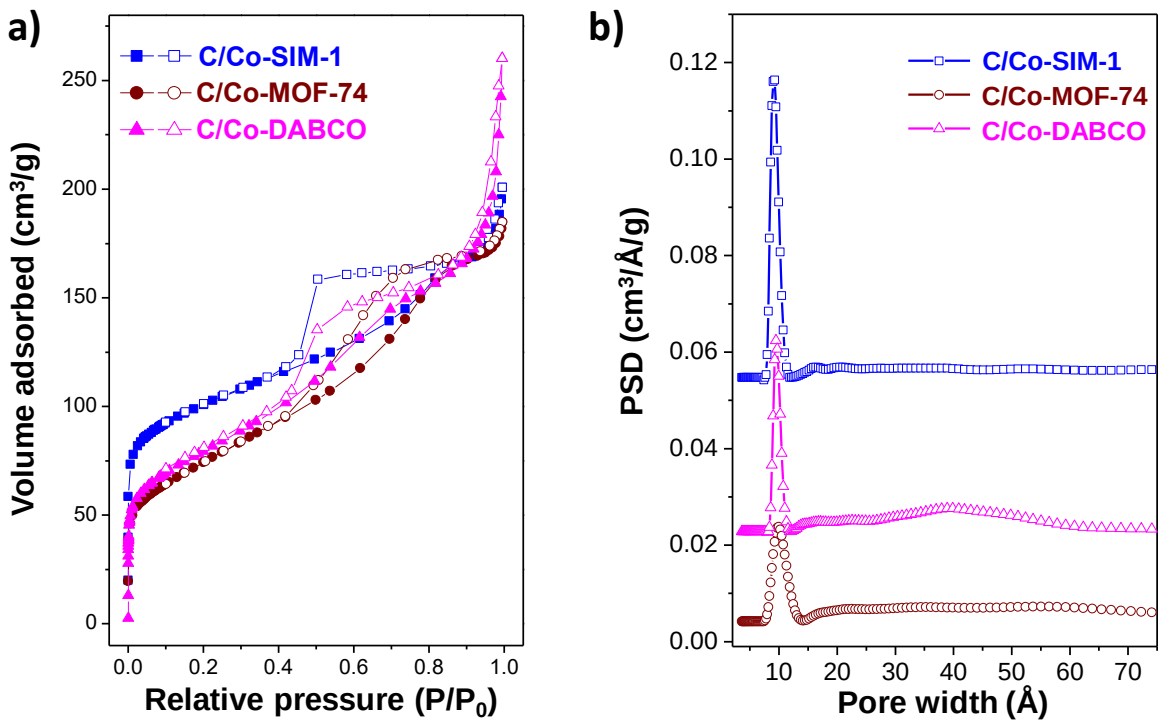

Fig. 3. (a) N_2 adsorption-desorption isotherms and (b) pore size distributions of C/Co-SIM-1, C/Co-MOF-74 and C/Co-DABCO samples.

Table 1. Textural properties of C/Co-SIM-1, C/Co-MOF-74 and C/Co-DABCO samples.

Sample	S_{BET} (m^2/g)	V_p (cm^3/g)	Pore width (Å)
C/Co-SIM-1	361	0.25	8-10/14-100
C/Co-MOF-74	261	0.24	8-13/15-90
C/Co-DABCO	291	0.25	9-11/14-65

To study the nature of the carbon formed during the carbonization process, Raman spectra of the samples were recorded. As shown in Fig. 4a, all the carbon samples exhibited two broad bands near 1310 and 1581 cm^{-1} which correspond to the D and G bands of the carbon, respectively. D band is attributed to the presence of defects or disorder within the carbon, and the G band is associated with the sp^2 hybridization existing in graphitic carbon.[33] The relative intensity ratio between D and G band (I_D/I_G) in the Raman spectra provides useful

information about the graphitization degree of the carbonaceous materials.[34] The I_D/I_G ratios calculated for C/Co-SIM-1, C/Co-MOF-74 and C/Co-DABCO were 2.21, 1.78 and 1.55, respectively, indicating that the prepared carbons possessed mainly disorder structures or contained long-range disordered graphitic carbon, being the C/Co-SIM-1 the carbon which presented more quantity of defects. X-ray photoelectron spectroscopy (XPS) analysis of the MOFs derived carbons was performed to investigate their chemical composition. In all cases, the spectra (Fig. 4b) exhibit peaks in the C 1s, Co 2p and O 1s regions, which confirm the presence of these elements in all the materials. Additionally, the spectra of C/Co-SIM-1 and C/Co-DABCO showed a signal in the N 1s region, indicating the presence of N in both samples coming from the ligands used for their synthesis. For all the materials the high-resolution C 1s spectra (Fig. S3) showed two peaks centered at 284.5 eV and 288.5 eV, which are assigned to C–C/C=C and C=O bonds, respectively.[35,36] The spectra in the Co 2p region of C/Co-SIM-1, C/Co-MOF-74 and C/Co-DABCO (Fig. S4) are fitted to six peaks corresponding to metallic cobalt (794.8 eV - 793.8 eV and 779.6 eV - 778.6 eV), cobalt oxide (796.8 eV – 796.4 eV and 781.2 eV – 780.6 eV) and shake-up satellite peaks (803.8 eV – 803.0 eV and 785.8 eV – 785.0 eV).[35,37,38] The spectra N 1s of C/Co-SIM-1 and C/Co-DABCO (Fig. S5) showed three signals centered at 398.6, 400.7 and 405.4 eV, which can be assigned to pyridinic N, graphitic N and oxidized N, respectively.[39]

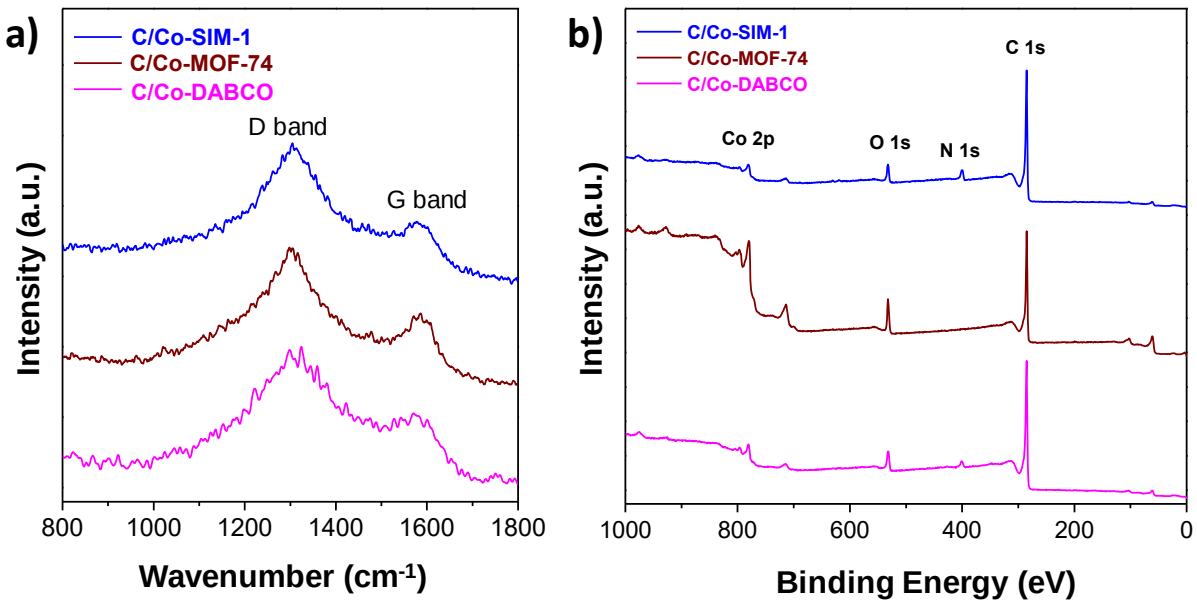

Figure 4. (a) Raman and (b) XPS spectra of C/Co-SIM-1, C/Co-MOF-74 and C/Co-DABCO samples.

3.2 Extraction of sulfonamides

Carbons derived from cobalt (II)-based metal-organic frameworks were tested for the simultaneous magnetic extraction of three sulfonamides (sulfadiazine, sulfamerazine and sulfametazine). Fig. 5 shows the percentages of sulfonamides adsorbed by the three prepared carbons from a 5 mg L^{-1} (each) solution. As it can be observed, the three MOF-derived carbons showed high extraction percentages, which are comparable or even better than most of the values reported in the literature using other magnetic adsorbents,[40–42] especially in the case of C/Co-SIM-1 carbon which reaches values higher than 95%. The excellent adsorption performance of this material could be attributed to its higher surface area and bimodal pore structure, which facilitates the access of sulfonamides to the pores, and its significant amount of surface defects, which could act as adsorption sites of SNs, improving the extraction

capacity.[36] According to these results, the C/Co-SIM-1 was selected for the study of the extraction variables.

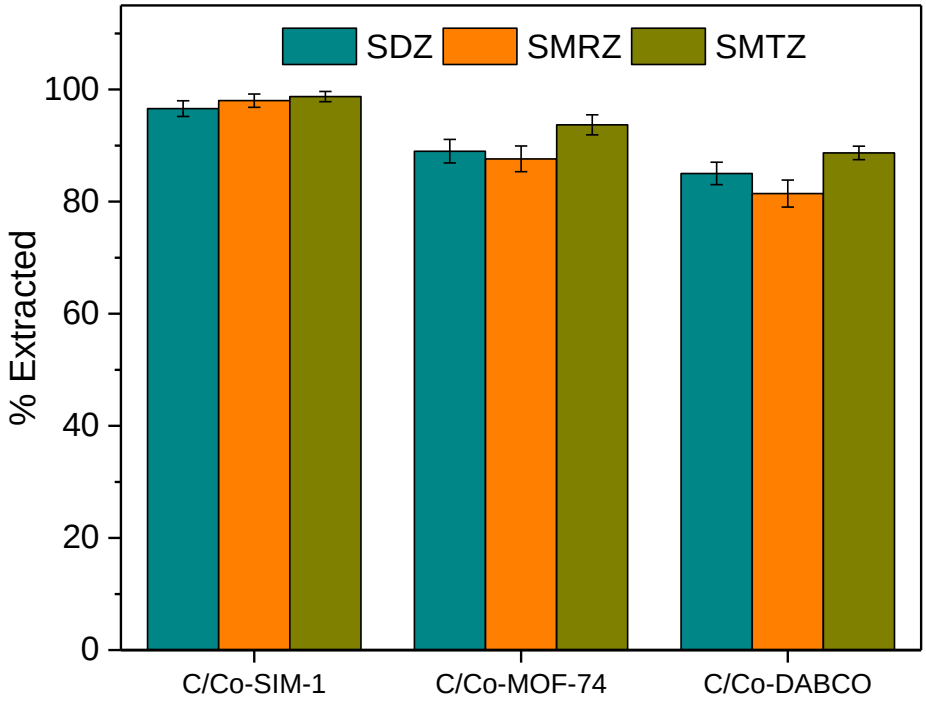

Fig. 5. Percentage of sulfonamides extracted by C/Co-SIM-1, C/Co-MOF-74 and C/Co-DABCO samples.

The leaching of cobalt ions into the water after the adsorption experiments using C/Co-SIM-1 was studied by inductively coupled plasma optical emission spectrometry (ICP-OES). After 2 h in solution, a small amount of cobalt was detected in the supernatant solution, which remained constant with the time, indicating that after the carbonization treatment of the MOF a small quantity of cobalt is not well attached to the carbon matrix. To eliminate it, the carbon sample was washed with water before the extraction experiments.

Taking into account that the pH of the solution influences adsorption, since it determines the surface charge of adsorbent and the speciation of the adsorbate, the extraction of

sulfonamides by the C/Co-SIM-1 carbon was carried out at different pH values (Fig. S6). As it can be observed, the highest extraction percentages for the three SNs were achieved at pH values between 5 and 7.5 and the adsorption capacity significantly decreased when the pH increased from 7.5 to 10. Considering the pKa values of the studied sulfonamides[4] and the isoelectric point of C/Co-SIM-1 (Fig. S7), it must exist an electrostatic attraction between the negatively charged surface of the carbon material and the positively charged SNs at weak acid and neutral pH, which becomes a repulsion in basic conditions due to the negative charge of SNs at high pH values. However, the high extraction capacity of C/Co-SIM-1, even at basic pH, suggests that other mechanisms, such as π- π interactions and hydrogen bonding, should exist between the carbon and the sulfonamides.[10,43]

The effect of the contact time on the adsorption of SDZ, SMRZ and SMTZ on C/Co-SIM-1 was also studied (Fig. S8). For the three sulfonamides, the adsorption equilibrium was reached in 30 min, indicating a fast extraction process. The adsorption kinetic data were analyzed using a pseudo-second-order kinetic model;[25] the fitting results are presented in Table 2. The obtained determination coefficients (R^2), which were between 0.9916 and 0.9932, indicate that the experimental data could be successfully fitted by this model, suggesting that chemical adsorption is the rate-limiting step of the adsorption process and it is dependent on the number of active sites.[8] The amount of each of the sulfonamides adsorbed at equilibrium ranks among the highest ones reported in the literature using magnetic adsorbents, demonstrating the high adsorption capacity of C/Co-SIM-1,[44–49] probably related to its high surface area and porosity and the different interactions that could take place between the adsorbent and the target analytes.

Table 2. Parameters of the pseudo-second-order kinetic model for the SNs adsorption by C/Co-SIM-1 carbon.

SNs	$q_{e(exp)}$ (mg/g)	Pseudo-second-order kinetic model		
		$q_{e(calc)}$ (mg/g)	k_2 (g/mg min)	R^2
SDZ	48.21	44.44	0.00111	0.9916
SMRZ	48.85	45.04	0.00113	0.9932
SMTZ	49.51	45.66	0.00112	0.9931

In order to study the applicability of the C/Co-SIM-1 carbon, we evaluated its capacity for the simultaneous extraction and preconcentration of sulfonamides from water. Fig. 6 shows the chromatograms obtained, before and after solid-phase extraction, of the three sulfonamides from a mixture solution of 5 mg/L each, using C/Co-SIM-1 as adsorbent and 1 mL of methanol as eluent. It can be seen that the intensity of the SNs peaks significantly increases after preconcentration, reaching enrichment factors of 47, 43 and 44 for SDZ, SMRZ and SMTZ, respectively, in comparison with the direct injection of a mixture of sulfonamides.

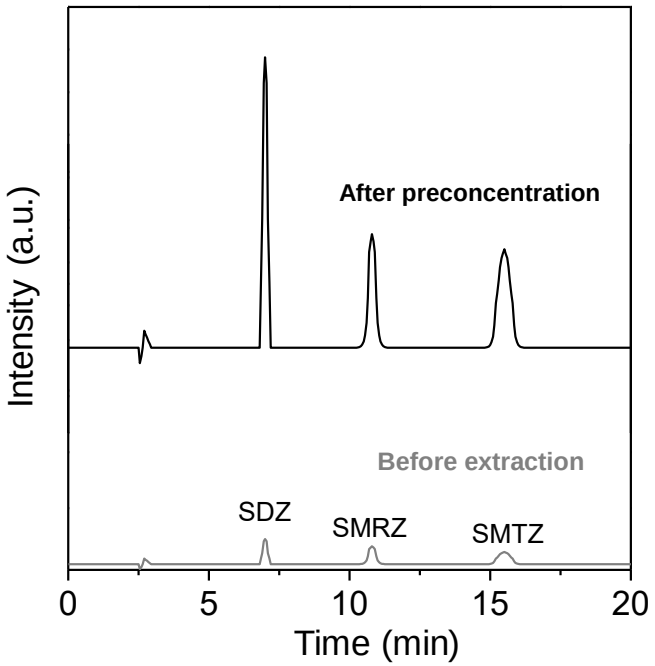

Fig. 6. SDZ, SMRZ and SMTZ chromatograms before and after solid-phase extraction by using C/Co-SIM-1.

An important feature for practical extraction applications is the reusability of the adsorbent. To evaluate the capacity of regeneration of the C/Co-SIM-1 material, a recyclability extraction test during five consecutive cycles was carried out. As it can be observed in Fig. 7, after 5 extraction cycles, similar extraction capacities of the three sulfonamides were obtained. The relative standard deviations of the extraction capacity of SDZ, SMRZ and SMTZ were 1.5, 2.1 and 1.0%, respectively, demonstrating the excellent reusability of C/Co-SIM-1 for the extraction of sulfonamides.

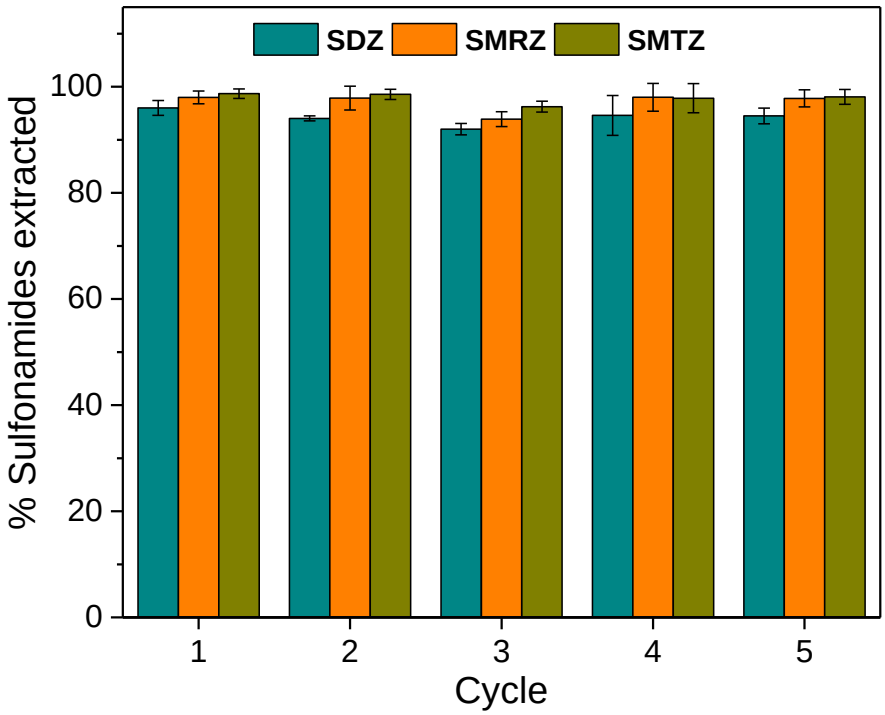

Figure 7. Recyclability of C/Co-SIM-1 for adsorption of SNs from water.

4. Conclusions

In this study, the use of magnetic porous carbons derived from metal-organic frameworks as sorbents for solid-phase extraction of sulfonamides has been explored for the first time. Three different cobalt(II)-based MOFs: Co-SIM-1, Co-MOF-74 and Co-DABCO, were used as precursors for the preparation of highly porous magnetic carbons via a simple carbonization process. These magnetic carbons were used for the dispersive solid-phase extraction of sulfamethazine, sulfamerazine and sulfadiazine avoiding tedious filtration or centrifugation steps. The highest SNs extraction performance was reached with C/Co-SIM-1 carbon, due to its large number of surface defects, high surface area and bimodal pore structure which facilitated the SNs adsorption on the internal channels of this material. The C/Co-SIM-1

exhibited fast extraction kinetics and high enrichment factors ranging from 43 to 47 for the mixture of three sulfonamides catalogued as emerging contaminants. The obtained C/Co-SIM-1 carbon was reused several times keeping its extraction performance, making it a promising material for the simultaneous extraction and preconcentration of emerging pollutants from water.

5. Acknowledgements

The authors acknowledge Spanish Agencia Estatal de Investigación (AEI) and European Funds for Regional Development (FEDER) for financial support through Project CTQ2016-77155-R (AEI/FEDER, UE). Mendiola-Alvarez thanks to CONACYT and to Centro de Estudios de Posgrado (UIB) for the scholarship support. The authors acknowledge F. Hierro Riu for scanning micrographs.

6. References

1. Y. Liu, J. Wang, *J. Hazard Mater*., 2013, **250–251**, 99–105.
2. M. García, M. Villagrasa, M. Díaz, D. Barceló, *Anal. Bioanal. Chem*., 2010, **397**, 1325–1334.
3. K. Ikehata, N. Jodeiri, M. Gamal, *Ozone Sci. Eng*., 2006, **28**, 353–414.
4. Y. Ma, K. Zhang, C. Li, T. Zhang, N. Gao, *Biomed. Res. Int*., 2015, **2015**, 1–10.
5. A. Batt, D. Snow, D. Aga, *Chemosphere*, 2006, **64**, 1963–1971.
6. Q. Jiuhui, *J. Environ. Sci*., 2008, **20**, 1–13.
7. A. Mansoor, M. Lashgari, *Chem. Eng. J*., 2009, **150**, 555–560.
8. Y. Gao, R. Kang, J. Xia, G. Yu, S. Deng, *J. Colloid Interface Sci*., 2019, **535**, 159–168.
9. M. Azhar, H. Abid, V. Periasamy, H. Sun, M. Tade, S. Wang, *J. Colloid Interface Sci*., 2017, **500**, 88–95.

10. S. Hasan, A. Easley, M. Beth, B. Monroe, D. Maitland, *J. Colloid Interface Sci*., 2016, **478**, 334–343.

11. Y. Shih, K. Wang, B. Singco, C. Lin, H. Huang, *Langmuir*, 2016, **32**, 11465–11473.

12. B. Hashemi, P. Zohrabi, N. Raza, K. Kim, *TrAC - Trends Anal. Chem*., 2017, **97**, 65–82.

13. S. Yang, T. Kim, J. Im, Y. Kim, K. Lee, H. Jung, C. Park, *Chem. Mater*., 2012, **24**, 464–470.

14. L. Yang, X. Zeng, W. Wang, D. Cao, *Adv. Funct. Mater*., 2018, **28**, 1704537.

15. C. Palomino Cabello, M. Picó, F. Maya, M. del Rio, G. Turnes Palomino, *Chem. Eng. J*., 2018, **346**, 85–93.

16. B. Bhadra, S. Jhung, *Microporous Mesoporous Mater*., 2018, **270**, 102–108.

17. A. Banerjee, R. Gokhale, S. Bhatnagar, J. Jog, M. Bhardwaj, B. Lefez, *J. Mater. Chem*., 2012, **22**, 19694–19699.

18. L. Wang, F. Ke, J. Zhu, *Dalt. Trans*., 2016, **45**, 4541–4547.

19. Y. Liu, Z. Gao, R. Wu, Z. Wang, X. Chen, T. Chan, *J. Chromatogr. A*, 2017, **1479**, 55–61.

20. F. Maya, C. Palomino Cabello, R. Frizzarin, J. Estela, G. Turnes Palomino, V. Cerdà, *TrAC - Trends Anal. Chem*., 2017, **90**, 142–152.

21. S. Zhang, Q. Yang, Z. Li, W. Wang, C. Wang, Z. Wang, *Analyst*, 2016, **141**, 1127–1135.

22. S. Aguado, J. Quirós, J. Canivet, D. Farrusseng, K. Boltes, R. Rosal, *Chemosphere*, 2014, **113**, 188–192.

23. H. Cho, D. Yang, J. Kim, S. Jeong, W. Ahn, *Catal. Today*, 2012, **185**, 35–40.

24. L. Gómez, S. Castro, M. Sánchez, S. Yáñez-, J. Mira, J. Bermúdez, T. Centeno, M. Señarís, *Eur. J. Inorg. Chem*., 2016, **2016**, 4463–4469.

25. Y. Ho, G. McKay, *Process Biochem*., 1999, **34**, 451–465.

26. N. Rosi, J. Kim, M. Eddaoudi, B. Chen, M. O'Keeffe, O. Yaghi, *J. Am. Chem. Soc*., 2005, **127**, 1504–1518.

27. X. Li, C. Zeng, J. Jiang, L. Ai, *J. Mater. Chem. A*, 2016, **4**, 7476–7482.

28. N. Torad, M. Hu, S. Ishihara, H. Sukegawa, A. Belik, M. Imura, K. Ariga, Y. Sakka, Y. Yamauchi, *Small*, 2014, **10**, 2096–2107.

29. S. Chen, L. Wen, F. Svec, T. Tan, Y. Lv, *RSC Adv*., 2017, **7**, 21205–21213.

30. Z. Yu, X. Wang, Y.-N. Hou, X. Pan, Z. Zhao, J. Qiu, *Carbon*, 2017, **117**, 376–382.

31. S. Dang, Q. Zhu, Q. Xu, Nat. Rev. Mater., 2018. **3**, 17075.

32. M. Thommes, K. Kaneko, A. Neimark, J. Olivier, F. Rodriguez, J. Rouquerol, K. Sing, *Pure Appl. Chem*., 2015, **87**, 1051–1069.

33. C. Zhang, N. Mahmood, H. Yin, F. Liu, Y. Hou, *Adv. Mater*., 2013, **25**, 4932–4937.

34. B. Chen, G. Ma, Y. Zhu, Y. Xia, *Sci. Rep*., 2017, **7**, 1–9.

35. C. Cui, Z. Wei, G. Zhou, W. Wei, J. Ma, L. Chen, C. Li, *J. Mater. Chem. A*, 2018, **6**, 7088–7098.

36. Q. Wang, L. Zhang, *J. Chromatogr. A*, 2018, **1568**, 1–7.

37. S. Das, M. Bhunia, M. Motin, S. Dutta, A. Bhaumik, *Dalt. Trans*., 2011, **40**, 2932–2939.

38. H. Lu, H. Zhang, R. Liu, X. Zhang, H. Zhao, G. Wang, *Appl. Surf. Sci*., 2017, **392**, 402–409.

39. L. Wang, S. Dou, J. Xu, H. Liu, S. Wang, J. Ma, S. Dou, *Chem. Commun*., 2015, **51**, 11791–11794.

40. H. Wu, Y. Shi, X. Guo, S. Zhao, J. Du, H. Jia, L. He, L. Du, *J. Sep. Sci.*, 2016, **39**, 4398–4407.

41. p-S. Gao, Y. Guoa, X. Lia, X. Wang, J. Wang, F. Qian, H. Gu, Z. Zhang, *J. Chromatogr. A*, 2018, **1575**, 1–10.

42. Y. Zhao, R. Wu, H. Yu, J. Li, L. Liu, S. Wang, X. Chen, T.-W. D. Chan, *J. Chromatogr. A*, 2020, **1610**, 460543.

43. M. Teixidó, J. Pignatello, J. Beltrán, M. Granados, J. Peccia, *Environ. Sci. Technol*., 2011, **45**, 10020–10027.

44. P. Shi, N. Ye, *Anal. Methods*, 2014, **6**, 9725–9730.

45. M. Izanloo, A. Esrafili, M. Behbahani, M. Ghambarian, H. Reza Sobhi, *J. Sep. Sci.*, 2018, **41**, 910–917.

46. Y. Li, N. Zhu, T. Chen, Y. Ma, Q. Li, *Microchem. J*., 2018, **138**, 401–407.

47. J. Zhang, Z. Chen, S. Tang, X. Luo, J. Xi, Z. He, J. Yu, F. Wu, *Anal. Chim. Acta*, 2019, **1089**, 66–77.

48. J.-M. Liu, S.-W. Lv, X.-Y. Yuan, H.-L. Liu, S. Wang, *RSC Adv.*, 2019, **9**, 14247–14253.

49. Z. Chen, Z. He, X. Luo, F. Wu, S. Tang, J. Zhang, *Food Anal. Method*, 2020, https://doi.org/10.1007/s12161-020-01750-2.

438

439

440

441

442

443

444

445

446

447

448

449

450

451

452

453